

University of Warwick institutional repository: <http://go.warwick.ac.uk/wrap>

This paper is made available online in accordance with publisher policies. Please scroll down to view the document itself. Please refer to the repository record for this item and our policy information available from the repository home page for further information.

To see the final version of this paper please visit the publisher's website. Access to the published version may require a subscription.

Author(s): Zhenjun Wang, Yuanjia Hong, Jinke Tang, Cosmin Radu, Yuxi Chen, Leonard Spinu, Weilie Zhou, and Le Duc Tung

Article Title: Giant negative magnetoresistance of spin polarons in magnetic semiconductors—chromium-doped Ti_2O_3 thin

Year of publication: 2005

Link to published version: <http://dx.doi.org/10.1063/1.1874302>

Publisher statement: None

Giant negative magnetoresistance of spin polarons in magnetic semiconductors—chromium-doped Ti_2O_3 thin films

Zhenjun Wang, Yuanjia Hong, and Jinke Tang^{a)}

Department of Physics, University of New Orleans, New Orleans, Louisiana 70148

Cosmin Radu, Yuxi Chen, Leonard Spinu, and Weillie Zhou

Advanced Materials Research Institute, University of New Orleans, New Orleans, Louisiana 70148

Le Duc Tung

Department of Physics, University of Warwick, Coventry CV4 7AL, United Kingdom

(Received 23 April 2004; accepted 11 January 2005; published online 18 February 2005)

Epitaxial Cr-doped Ti_2O_3 films show giant negative magnetoresistance up to -365% at 2 K. The resistivity of the doped samples follows the behavior expected of spin (magnetic) polarons at low temperature. Namely, $\rho = \rho_0 \exp(T_0/T)^p$, where $p=0.5$ in zero field. A large applied field quenches the spin polarons and p is reduced to 0.25 expected for lattice polarons. The formation of spin polarons is an indication of strong exchange coupling between the magnetic ions and holes in the system. © 2005 American Institute of Physics. [DOI: 10.1063/1.1874302]

Dilute magnetic semiconductors have attracted much attention recently because of their combined magnetic and transport properties. In such materials, the current carriers are either strongly coupled to local moments of the magnetic atoms or directly participate in the magnetism themselves. Among TiO_2 -related materials, experimental results have shown evidence of room-temperature ferromagnetism in Co-doped anatase TiO_2 ,^{1,2} Fe-doped reduced-rutile $\text{Ti}_n\text{O}_{2n-1}$,³ and Co/Fe-doped $\text{SnO}_{2-\delta}$ (Refs. 4 and 5) thin films. Several models, including Zener-type Ruderman–Kittel–(Kasuya)–Yosida, double exchange, and spin-polarons, have been proposed to explain the room-temperature ferromagnetism although its exact origin is unclear. We have recently investigated the magnetic properties of Cr-doped Ti_2O_3 thin films and report in this letter on giant negative magnetoresistance (MR) due to spin (magnetic) polaron formation at low temperatures.

Ti_2O_3 has a corundum ($\alpha\text{-Al}_2\text{O}_3$) structure. Below 200 °C, Ti_2O_3 is a nonmagnetic semiconductor, with an energy gap ($E_G \sim 0.1$ eV) between the top of a_{1g} band and the bottom of e_g bands of the $3d$ electrons. The electrons in the conduction band are much heavier than the holes in the valence band, and the material exhibits a positive Hall coefficient (p type). Long ago, Mott suggested that the excited carriers in Ti_2O_3 are small polarons. Low-temperature conductivity shows $\exp(-T_0/T)^p$ ($p=0.25$) temperature dependence consistent with the variable range hopping (VRH) nature of the polaron transport.⁶

$(\text{Cr}_x\text{Ti}_{1-x})_2\text{O}_3$ ($x=0, 0.04, 0.06,$ and 0.10) thin films were grown on $\alpha\text{-Al}_2\text{O}_3(012)$ substrates by pulsed-laser deposition. Prescribed amounts of high-purity TiO_2 and Cr powders were mixed, cold pressed, and sintered to make a $\text{Cr}_x\text{Ti}_{1-x}\text{O}_2$ ceramic target. The films were prepared in a vacuum of 2×10^{-6} Torr at substrate temperatures of 800–1000 K. The pulsed excimer laser uses KrF($\lambda=248$ nm) and produces a laser beam of intensity of $1\text{--}2$ J/cm² and repetition rate of 4 Hz. The deposition rate is

between 0.3 and 0.5 Å/s, and the film thickness varies from 150 nm to 300 nm. Single-phase epitaxial $(\text{Cr}_x\text{Ti}_{1-x})_2\text{O}_3$ films were formed by ablating the $\text{Cr}_x\text{Ti}_{1-x}\text{O}_2$ targets and reduction during the deposition.

The x-ray diffraction (XRD) and transmission electron microscopy (TEM) results show that the $(\text{Cr}_x\text{Ti}_{1-x})_2\text{O}_3$ films are single phase. Figure 1 (inset) shows the XRD patterns of $(\text{Cr}_{0.10}\text{Ti}_{0.90})_2\text{O}_3$ and Ti_2O_3 films grown on $\alpha\text{-Al}_2\text{O}_3$. Only the reflections from the (012) family of corundum phase are observed. The Cr content dependence of the R -axis lattice spacing [$d(012)$] is shown in Fig. 1. The value of $d(012)$ decreases linearly with the Cr concentration, indicating that the Cr ions gradually substitute for the Ti ions in the films without changing the corundum structure. The Cr concentrations of the films were measured with energy dispersive x-ray spectroscopy in TEM mode, and they were consistent with those of the targets.

Figure 2 shows the magnetization M curves for $(\text{Cr}_{0.06}\text{Ti}_{0.94})_2\text{O}_3$ at 2 K and 300 K. The magnetization of $(\text{Cr}_{0.06}\text{Ti}_{0.94})_2\text{O}_3$ at 2 K increases with the applied field and

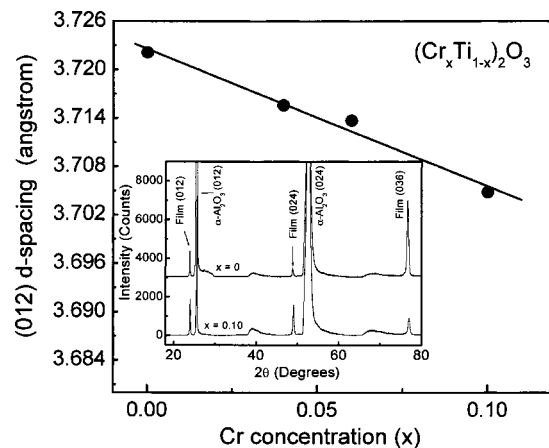


FIG. 1. The peak position of the (012) reflection of $(\text{Cr}_x\text{Ti}_{1-x})_2\text{O}_3$ films shifts to higher angles with increasing Cr concentration x . The $d(012)$ spacing decreases with x . Inset: XRD patterns for $(\text{Cr}_{0.10}\text{Ti}_{0.90})_2\text{O}_3$ and Ti_2O_3 films. Only the peaks of the (012) family of corundum phase are observed.

^{a)} Author to whom correspondence should be addressed; electronic mail: jtang@uno.edu

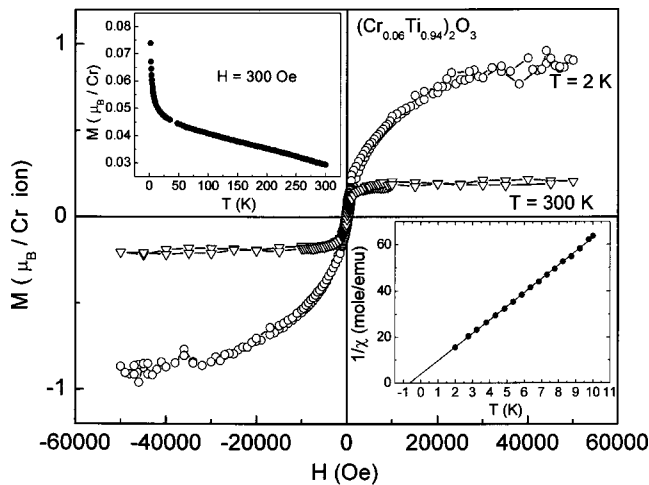


FIG. 2. Magnetization vs field curves of $(\text{Cr}_{0.06}\text{Ti}_{0.94})_2\text{O}_3$ film measured with a superconducting quantum interference device at $T=2$ K and 300 K. The upper-left-hand side inset shows the temperature dependence of the magnetization measured at $H=300$ Oe. The Curie-Weiss behavior at low temperature, after subtraction of the ferromagnetic component, is shown in the lower-right-hand side inset.

does not reach saturation at 50 kOe. It apparently consists of two components. One is a low-field ferromagnetic component, which shares the same origin as the ferromagnetic signals at high temperatures. The other is a paramagnetic component that corresponds to the upturn at low temperature in the $M-T$ curve (upper-left-hand side inset of Fig. 2). The moment at 2 K and 50 kOe is 0.5, 0.91 and 0.87 μ_B/Cr for $x=0.04$, 0.06, and 0.10, respectively. It initially increases with x , then decreases slightly upon a further increase in Cr doping. The room-temperature moments are much smaller, e.g., 0.2 μ_B/Cr for $x=0.06$. The origin of the room-temperature ferromagnetism is not clear and may be from magnetic impurities. The lower-right-hand side inset of Fig. 2 shows the Curie-Weiss behavior of the susceptibility at low temperature after the ferromagnetic component is subtracted. A negative paramagnetic Curie temperature ($\theta=-0.6$ K) suggests an antiferromagnetic ground state for the system.

In Fig. 3, we compare the temperature dependence of

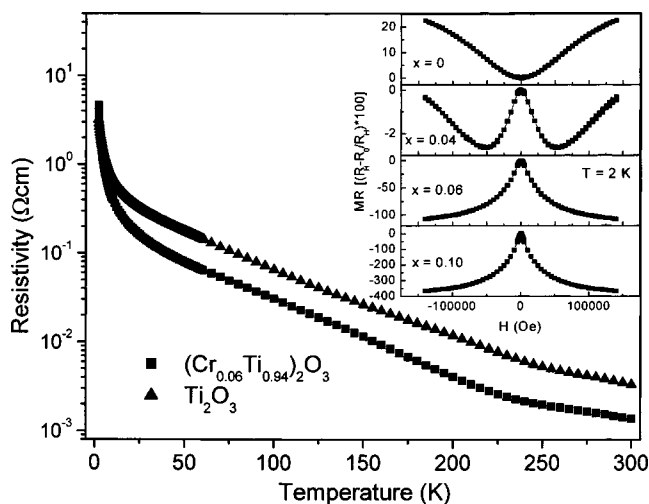


FIG. 3. The temperature dependence of the resistivity for the films, showing semiconducting behavior. Insets show MR curves for Ti_2O_3 and $(\text{Cr}_x\text{Ti}_{1-x})_2\text{O}_3$ at 2 K.

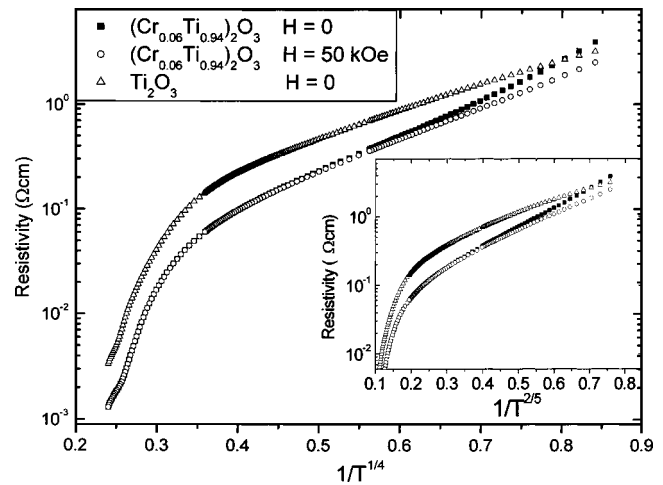


FIG. 4. The resistivity in logarithmic scale of as a function of $1/T^{0.25}$. The data were taken in zero field for Ti_2O_3 and in $H=0$ and 50 kOe for $(\text{Cr}_{0.06}\text{Ti}_{0.94})_2\text{O}_3$. Inset shows $\ln \rho$ vs $1/T^{0.4}$ plots for the same three data sets.

resistivity for the undoped Ti_2O_3 and $(\text{Cr}_{0.06}\text{Ti}_{0.94})_2\text{O}_3$ films. The films exhibit increasing resistivity with decreasing temperature. The carriers are p type for both doped and undoped films. A carrier density of $1.2 \times 10^{21}/\text{cm}^3$ was estimated for $(\text{Cr}_{0.06}\text{Ti}_{0.94})_2\text{O}_3$ from the Hall measurements. All films show a rapid increase in resistivity at very low temperatures (below about 30–40 K), which is due to the VRH of polarons and spin polarons as will be discussed next.

The MR $(= (R_H - R_0)/R_H \times 100\%)$ was measured for Ti_2O_3 and $(\text{Cr}_x\text{Ti}_{1-x})_2\text{O}_3$ films. The upper-right-hand side inset of Fig. 3 shows the MR curves measured at 2 K. The MR for Ti_2O_3 is positive 23% at 140 kOe. This large positive MR is in agreement with previous data and is explained with a two-band model where both electrons and holes participate in the transport.⁷ For doped $(\text{Cr}_x\text{Ti}_{1-x})_2\text{O}_3$, the MR is negative and large. Sample $x=0.06$ has a giant value of -80% and -107% at 50 kOe and 140 kOe, respectively. The MR for $x=0.10$ reaches -365% at 140 kOe. For $x=0.04$, positive MR dominates in high fields. The MR correlates well with the magnetization shown in Fig. 2. Its giant negative values cannot be explained in the framework of scattering by magnetic impurities, scattering by magnetic granules, or magnetic tunneling between two granules. Rather, its origin lies in the quenching of spin (magnetic) polarons by the applied field, in which extremely large negative MR is expected and observed.⁸

We now discuss the origin of the giant negative MR in conjunction with the temperature dependence of the resistivity at low temperature. As mentioned at the beginning of this letter, Ti_2O_3 exhibits VRH conductance at low temperature and its resistivity follows an $\exp[1/T^{0.25}]$ behavior. Our undoped Ti_2O_3 film exhibits a slightly smaller exponent p of 0.12 as determined from a least-squares fit. The deviation from the expected value of 0.25 is not surprising considering the diverse values of p (0.18–0.7) seen for VRH in various materials.^{9,10} We have plotted the resistivity in logarithmic scale of Ti_2O_3 along with that of $(\text{Cr}_{0.06}\text{Ti}_{0.94})_2\text{O}_3$ as a function of $1/T^{0.25}$ in Fig. 4. The small departure from a linear behavior is noticeable. For doped $(\text{Cr}_{0.06}\text{Ti}_{0.94})_2\text{O}_3$, the resistivity in zero field does not follow $\exp(1/T)^{0.25}$ law as seen in the upturn at low temperatures. Instead, its resistivity was found to follow $\rho = \rho_0 \exp(T_0/T)^{0.4}$ at low temperature.

Figure 4 (inset) shows the resistivity of $(\text{Cr}_{0.06}\text{Ti}_{0.94})_2\text{O}_3$ in logarithmic scale as a function of $1/T^{0.4}$. A nearly perfect straight line is obtained. A least-squares fit gives an exponent of $p=0.391\pm 0.007$. This value is very close to 0.4 and is distinctively different from 0.5 expected for VRH with Coulomb blockade or tunneling transport in granular systems. The $1/T^{0.4}$ temperature dependence has been predicted by Foygel *et al.*¹¹ for bound spin (magnetic) polarons. Traditionally, spin polaron transport has been assumed to follow a simple activation process. Recent study demonstrates that, in the systems with significant disorder of magnetic energies, the spin polaron hopping also adopts a variable range nature and obeys $\rho=\rho_0 \exp(T_0/T)^p$ law, where $p=2/(d+2)$ and d is the dimensionality of the system. The thickness of our films (150–300 nm) falls into the $3d$ range, therefore $p=0.4$ is expected. The agreement between the spin polaron theory and our experimental data is excellent.

Further evidence for spin polaron transport comes from the resistivity data obtained in high magnetic field. The temperature dependence of the resistivity at $H=50$ kOe reverts back to the $\exp(T_0/T)^{0.25}$ behavior (see the linear behavior Fig. 4), suggesting that the spin polarons are quenched by high field and the transport returns to that of standard non-magnetic lattice polarons. An exponent $p=0.238\pm 0.005$ was obtained from the fit. The same data show negative curvature on a $\log R$ versus $1/T^{0.4}$ plot (Fig. 4, inset). In a field of 140 kOe, p was found to be 0.284 ± 0.001 . All data analysis and curve fitting were done over the temperature range 2 K $< T < 15$ K. The crossover from $p=0.4$ for magnetic polarons to $p=0.25$ for standard Mott lattice polarons in high magnetic field has been predicted in Ref. 11. It should be mentioned that the observed field dependence of exponent p is unique for magnetic polarons. The opposite trend in the field dependence of p is expected for lattice polaron VRH, where p generally increases from 0.25 in zero field to 0.33 in high fields in the absence of Coulomb interaction.¹²

The giant negative MR observed in $(\text{Cr}_x\text{Ti}_{1-x})_2\text{O}_3$ is characteristic of bound spin polarons. Bound spin polaron or bound magnetic polaron is the characteristic collective state of diluted magnetic semiconductors.¹³ Exchange interaction of localized carriers (holes) with magnetic Cr ions leads to the formation of bound spin polarons, which consists of the localized hole and surrounding cloud of Cr spins polarized via the exchange interaction. Without a magnetic field, the spin polarons have to move through the sea of Cr with somewhat randomly oriented spins. Their motion involves flipping many Cr spins, making the polarons massive and immobile.

With the field applied, all Cr spins are increasingly aligned to the direction of the field, which increases the mobility of the polarons.

In conclusion, our experiments show spin polaron formation in Cr-doped Ti_2O_3 films at low temperatures. The Cr-doped films exhibit giant negative MR as large as -365% at ~ 2 K, which is in contrast to the positive MR in the undoped film. The giant negative MR is indicative of the spin polaron formation. Analysis of the temperature dependence of the resistivity both in zero field and in high fields confirms the spin polaron interpretation of the data. The formation of spin polarons reveals the strong exchange coupling between the magnetic ions and the holes. It shows that Cr-doped Ti_2O_3 is a magnetic semiconductor where the carriers participate in the magnetism. We wish to note that spin polarons may provide a mechanism for the room-temperature ferromagnetism in doped semiconductors reported recently. Giant negative MR has been reported in the well-established ferromagnetic semiconductor (Ga,Mn)As and explained on the basis of bound magnetic polarons.¹⁴

This work was supported by Sharp Laboratories of America and by the Louisiana Board of Regents Support Fund (Grant No. LEQSF(2004-07)-RD-B-12).

¹Y. Matsumoto, M. Murakami, T. Shono, T. Hasegawa, T. Fukumura, M. Kawasaki, P. Ahmet, T. Chikyow, S. Koshihara, and H. Koinuma, *Science* **291**, 854 (2001).

²S. A. Chambers, *Mater. Today* **5**, 34 (2002); S. A. Chambers, S. Thevuthasan, R. F. C. Farrow, R. F. Marks, J. U. Thiele, L. Folks, M. G. Samant, A. J. Kellock, N. Ruzycski, D. L. Ederer, and U. Diebold, *Appl. Phys. Lett.* **79**, 3467 (2001).

³Z. Wang, W. Wang, J. Tang, L. Duc Tung, L. Spinu, and W. Zhou, *Appl. Phys. Lett.* **83**, 518 (2003).

⁴S. B. Ogale, R. J. Chouhary, J. P. Buban, S. E. Lofland, S. R. Shinde, S. N. Kale, V. N. Kulkarni, J. Higgins, C. Lanci, J. R. Simpson, N. D. Browning, S. Das. Sarma, H. D. Drew, R. L. Greene, and T. Venkatesan, *Phys. Rev. Lett.* **91**, 077205 (2003).

⁵J. M. D. Coey, A. P. Douvalis, C. B. Fitzgerald, and M. Venkatesan, *Appl. Phys. Lett.* **84**, 1332 (2004).

⁶J. Dumas and C. Schlenker, *J. Phys.* **37**, C4-41 (1976).

⁷J. M. Honig, *Rev. Mod. Phys.* **40**, 748 (1968).

⁸A. G. Petukhov and M. Foygel, *Phys. Rev. B* **62**, 520 (2000).

⁹R. M. Hill, *Phys. Status Solidi A* **35**, K29 (1976).

¹⁰A. G. Zabrodskii, *Sov. Phys. Semicond.* **11**, 345 (1977).

¹¹M. Foygel, R. D. Morris, and A. G. Petukhov, *Phys. Rev. B* **67**, 134205 (2003).

¹²M. Y. Azbel, *Phys. Rev. B* **43**, 2435 (1991).

¹³T. Dietl and J. Spalek, *Phys. Rev. Lett.* **48**, 355 (1982).

¹⁴F. Matsukura, H. Ohno, A. Shen, and Y. Sugawara, *Phys. Rev. B* **57**, R2037 (1998).